安全与电磁兼容
SAFETY & EMC

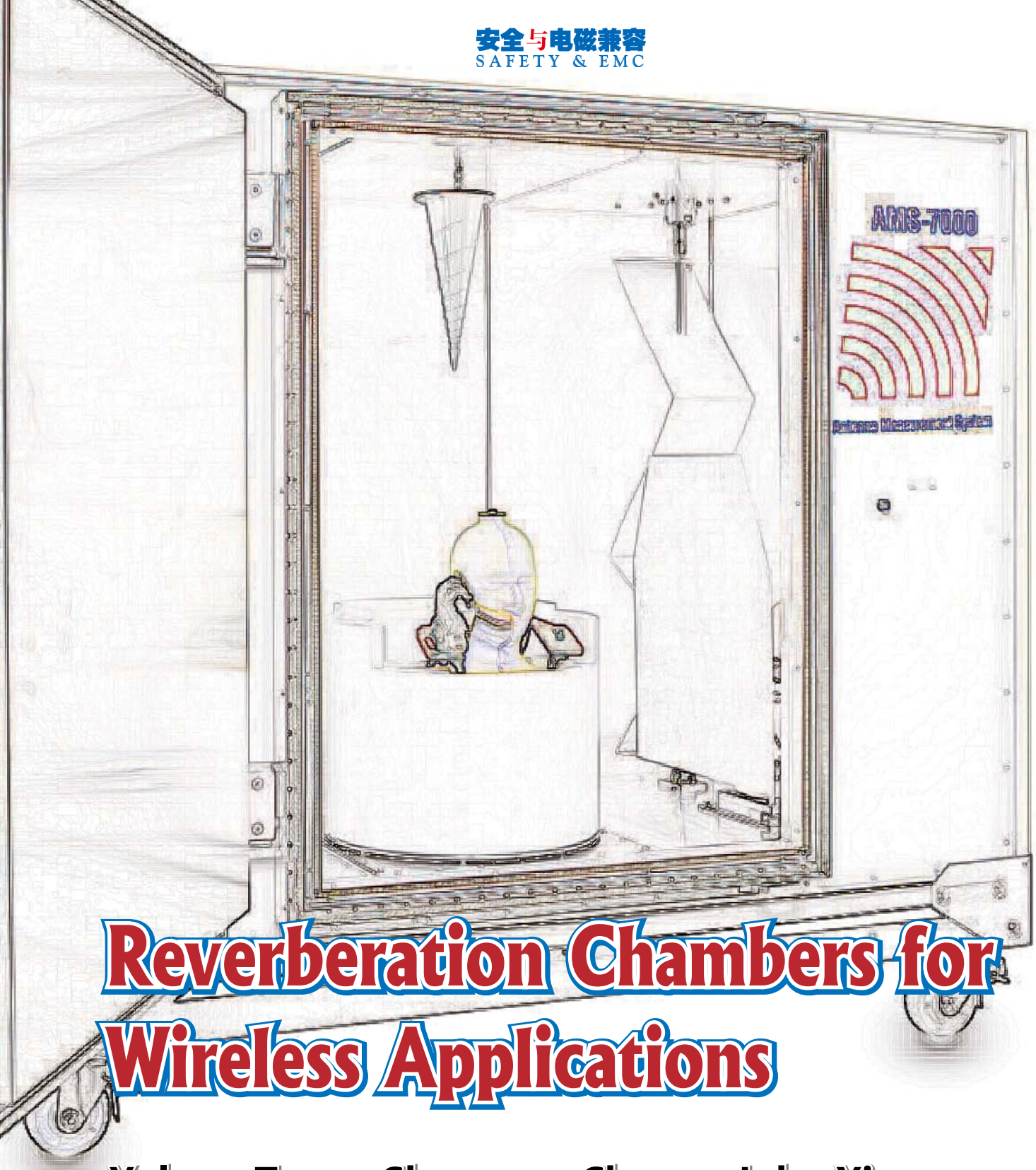

Reverberation Chambers for Wireless Applications

Yulung Tang, Shaoyang Cheng, John Xiao
ETS-Lindgren

Reprinted with permission of SAFETY & EMC Magazine from the 2014 SAFETY & EMC (English Edition)

Introduction

Owing to the beauty of its statistical behavior, reverberation chambers can be utilized as a measurement environment[1]. In a metallic cavity, numerous resonance modes can be excited. Each mode is induced by standing waves of the electrical fields that resonate with crests and troughs residing spatially. Such field variation due to resonance is seemingly contrary to the concept to establish a constant field with which the measurement can be repeated accurately inside the test volume. Repeatability is the key to the construction of a feasible measurement system. Although each individual resonance mode shows field deviation, the averaged field over sufficient modes can statistically achieve certain field uniformity that the measurement is then repeatable.

Initially, reverberation chambers were mainly implemented for radiated immunity testing for the capability of generating high field strength with less RF power than that in a conventional anechoic environment[2]. While not as prevalent as anechoic chambers, reverberation chambers were also used to measure radiated power and radiated sensitivity on wireless mobile devices[3]. However, the recent emergence of multiple-input, multiple-output (MIMO) technology, which takes advantage of multipath propagation to increase data throughput, has renewed interest in reverberation chambers for new wireless applications[4]. This is largely due to the fact of reverberation chambers inherently being a fading environment, a necessary component for testing MIMO devices. The resurgence of reverberation chambers in MIMO testing also brings the focus back to the use in conventional single-input, single-output (SISO) measurements, in which, as aforementioned, anechoic chambers have been previously dominant.

In different applications, either EMC or wireless, the main concept of using a reverberation chamber as a test environment does not change. Thus, this article starts with the introduction to the principle of reverberation chambers by studying the chamber transfer function in the first section, where both deductions from wave-like and mode-like points of view will be presented. In the second section, the practical implementation in SISO measurements with reverberation chambers will be described, while the third section serves the same purpose for MIMO measurements. At the end, the final section concludes the article with a glimpse of areas for future research involving reverberation chambers.

Chamber Transfer Function

Figure 1 illustrates a basic geometry of a reverberation system which is composed of the main metallic cavity with the stirrer and antennas inside the cavity. The stirrer, which can be one of multiple, rotates to generate a statistically uniform field. The two antennas are denoted as one for transmitting (TX) and the other for receiving (RX). The chamber transfer function (f_x) is the statistical average of the ratio of the received power to transmitted power. The denotation of the two antennas is fixed for the convenience of deducing f_x, although reciprocity holds in reverberation chambers[5], thus the chamber transfer function is indifferent if the TX and RX are reversed. Theoretically, if ideal statistical uniformity is achieved, the RF energy would then be all coupled through mode resonance, and the chamber transfer function will be independent of the locations of the TX and RX antennas. Practically, there will always be an amount of RF energy coupled directly from one antenna to the other. Thus, the locations of the antennas and the isolation between them are the factors to consider for designing a reverberation chamber. More details of reverberation chamber design will be described in the second section.

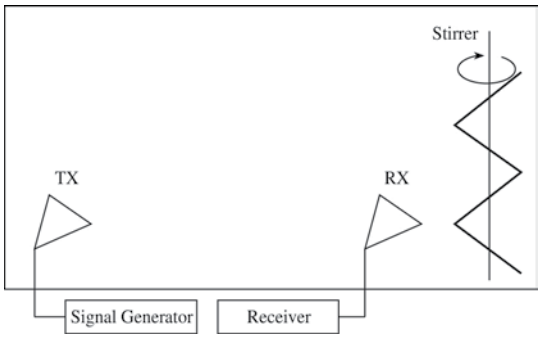

Figure 1 Illustration of a basic geometry of a reverberation chamber system

The chamber transfer function, as given in (1), for reverberation chambers has been described in several publications and is mainly deduced from wave perspective[6-8], which will be revisited in Part (A). The attempt to deduce the chamber transfer function from mode perspective will be given as well in Part (B). It will be shown that the deductions from both perspectives agree with each other.

$$f_x = \frac{P_R}{P_T} = \frac{\lambda^3 Q e_T e_R}{16\pi^2 V} \quad (1)$$

where P_R and P_T are the received and the transmitted powers, λ is the wavelength, Q is the quality factor, V is the cavity volume, e_T and e_R are antenna efficiencies for the TX antenna and the RX antenna.

Part (A) Wave Perspective

The chamber transfer function is simply the ratio of the

received power (P_R) to the transmitted power (P_T). From the wave perspective, the RX antenna collects RF power in proportion to its antenna effective area (A_E) and the surface power density (S_C), which is a function of the transmitted power P_T. Thus,

$$P_R = S_C(P_T)\cdot A_E \tag{2}$$

An ideal lossless cavity stores all the injected energy. Nonetheless, the cavity is made of the materials with finite conductivity, thus there is always energy dissipated in the cavity. Besides, for practical usage of a reverberation chamber, additional absorptive materials may be put inside the cavity to adjust the power delay constant. Quality factor (Q) is often used to describe such characteristic due to cavity loss. By definition, Q is the ratio of the stored cavity energy (U_C) to the dissipated power (P_D) per cycle. In the steady state, the stored energy is constant, and the injected power is equal to the dissipated power to compensate the power loss in each cycle, that is,

$$Q = \frac{\omega U_C}{P_T} \tag{3}$$

Given (3) and the cavity volume (V), the stored energy density (W_C) can be obtained as

$$W_C = \frac{P_T Q}{\omega V} \tag{4}$$

W_C is the volumetric density for energy, and S_C is the surface density for power. The energy density W_C transfers into the surface power density S_C with the speed of light c. Thus,

$$S_C = c\cdot W_C = \frac{CP_T Q}{\omega V} = \frac{F\lambda P_T Q}{2\pi f V} = \frac{\lambda P_T Q}{2\pi V} \tag{5}$$

With the surface power density given in (5), the received power P_R is then determined by its antenna effective area A_E, which can be expressed in terms of antenna gain (G) and wavelength (λ) as,

$$A_E = \frac{G\lambda^2}{4\pi} \tag{6}$$

In the steady state of the statistical uniformity, the antenna receives the same power isotropically, and the antenna gain is then taken as unity assuming that the antenna is lossless. In addition, the uniformity will spread power equality in each polarization, so the polarization mismatch factor of 1/2 needs to be applied. Thus, the effective antenna area is then rearranged as

$$A_E = \frac{\lambda^2}{8\pi} \tag{7}$$

The received power can be then calculated by applying (5) and (7) to (2)

$$P_R = \frac{\lambda P_T Q}{2\pi V}\cdot\frac{\lambda^2}{8\pi} \tag{8}$$

The ratio of P_R over P_T is obtained as follows

$$\frac{P_R}{P_T} = \frac{\lambda^3 Q}{16\pi^2 V} \tag{9}$$

Finally, with the efficiencies, e_T and e_R, of the TX and RX antennas being taken into account, the chamber transfer function can be obtained as the same as given in (2).

$$\frac{P_R}{P_T} = \frac{\lambda^3 Q e_T e_R}{16\pi^2 V} \tag{10}$$

Part (B) Mode perspective

From the mode perspective, the stored cavity energy U_C is uniformly distributed to each existing mode. The mode spectral density (N_f) is the total number of modes existing in the cavity at a given frequency (f). In the state of statistical uniformity, the RX antenna couples equal RF power via every single mode. Thus,

$$P_R = \frac{U_C}{N_f} \tag{11}$$

As described in Part (A), the cavity is lossy, so the quality factor defined in (3) applies here as well. According to (3) and (11), the chamber transfer function can be obtained as

$$\frac{P_R}{P_T} = \frac{Q}{\omega N_f} \tag{12}$$

Thus, the deduction of the chamber transfer function has become equivalent to that of the mode spectral density N_f for a given cavity volume V, three dimensions of which are L_1, L_2 and L_3.

In one dimension of confined length L_1, the resonance can only be excited as L_1 is an integer multiple of half wavelength. Thus the wavelength (λ_1) of the resonance modes must satisfy

$$\lambda_1 = \frac{2L_1}{n_1} \tag{13}$$

where n_1 is integer.

In the three dimensional cavity, the direction of the mode propagation is the wave number vector $\bar{K}$, which can be decomposed into three orthogonal components, $\bar{K}_1$, $\bar{K}_2$ and $\bar{K}_3$ The wavelength (λ) must satisfy

$$\bar{K} = \bar{K}_1 + \bar{K}_2 + \bar{K}_3 \text{ , then} \tag{14}$$

$$K^2 = K_1^2 + K_2^2 + K_3^2 \tag{15}$$

K is wave number, which is $2\pi/\lambda$. Regarding the resonance modeas one quantized particle, the satisfaction of (14) has the physical meaning that the particle bounces along the identical track inside the cavity. Expressed in terms of wavelength, (15) can be written as,

$$\frac{1}{\lambda^2} = \frac{1}{\lambda_1^2} + \frac{1}{\lambda_2^2} + \frac{1}{\lambda_3^2} \text{ , then} \tag{16}$$

$$\left(\frac{1}{\lambda}\right)^2 = \left(\frac{n_1}{2L_1}\right)^2 + \left(\frac{n_2}{2L_2}\right)^2 + \left(\frac{n_3}{2L_3}\right)^2 \tag{17}$$

where n_1, n_2, n_3 are integers.

(17) can viewed as the equation of a sphere surface with the

radius of $1/\lambda$. The total of excitable resonance modes is the number of possible integer solutions in the first octave, where n_1, n_2 and n_3 are all positive. The modes can be excited in either of the orthogonal polarizations, thus a factor of two will be applied as well. Thus, the total(N) of the excitable modes is

$$N = \frac{4}{3}\left(\frac{2L_1}{\lambda}\frac{2L_2}{\lambda}\frac{2L_3}{\lambda}\right)\cdot\frac{1}{8}(\text{one octant})\cdot 2(\text{two orthognal polarizations})$$

$$= \frac{8\pi}{3}\left(\frac{L_1L_2L_3}{\lambda^2}\right) = \frac{8\pi V}{3\lambda^2} = \frac{8\pi V f^2}{3C^2} = N(f) \tag{18}$$

Take the first derivative on $N(f)$ over frequency to obtain the mode spectral density N_f as follows.

$$N_f = \frac{\mathrm{d}N(f)}{\mathrm{d}f} = \frac{8\pi V f^2}{c^3} \tag{19}$$

Apply (19) onto (12), the chamber transfer function can be deduced as

$$\frac{P_R}{P_T} = \frac{Q}{\omega\frac{8\pi V f^2}{C^3}} = \frac{Q}{2\ f\frac{8\pi V f^2}{C^3}} = \frac{Q}{16\pi^2 V\frac{f^3}{C^3}} = \frac{\lambda^3 Q}{16\pi^2 V} \tag{20}$$

It is shown that (20) agrees with (9) where the deduction is carried out from wave-like perspective. Equation (10) can be formulized based on (20) as well after the efficiencies of the TX and RX antennas are taken into account. The agreement of the two deductions given in Part (A) and Part (B) provides the intuition that the designing of a reverberation chamber can be viewed from either wave-like or mode-like (particle-like) points of view.

Reverberation Chambers in a SISO Application

As a measurement system, there must be some quantity that is measureable and repeatable. The chamber transfer function deduced previously is such quantity that we can utilize it to carry out TRP (total radiated power) and TRS (total radiated sensitivity) measurements. However, the deduced chamber transfer function is based on the assumption that all the resonance modes are well stirred so that the statistical uniformity is achieved. Part (B) in the first section tells such perfect uniformity implies that the RF power is transferred from one location to the other, wherever the TX and RX antennas are located, all through resonance modes, every single one of which carries the same amount of RF power. In reality, perfect statistical uniformity does not exist but can be approached with deliberate designing of the system.

Figure 2 is the layout of a typical ETS-Lindgren AMS7000 reverberation chamber system which is illustrated herein to describe certain design concepts. The chamber dimension needs to be determined by the lowest operation frequency, such that there are still more than a hundred of modes that can be excited. In this case, the chamber dimensions of AMS7000 are 2.0 m tall, 1.5 m long and 1.2 m wide, and the lowest usable frequency is 700 MHz. There is a practical upper useable range as well due to wall losses, but it is higher than what is required for most wireless applications. The two stirrers are installed. The stirrers rotate during the measurement. From the particle-like perspective, the rotation of the stirrers provides various bouncing tracks of the particles, hence diversifying the resonance modes. The turntable, where the calibration antenna is located, rotates during the measurement to provide positioning stirring to the modes. There is a belt linking the vertical stirrer and the measurement antenna which is then rotated together with the vertical stirrer. The partition is used to block the direction energy coupling between the equipment under test (EUT) and the measurement antenna. Ideally, the chamber transfer function is independent of the locations of the antennas; in practicality, the statistical uniformity is optimized by minimizing the portion of the direction coupling. Thus, the two antennas are separated by a certain distance, and the partition is to provide additional isolation.

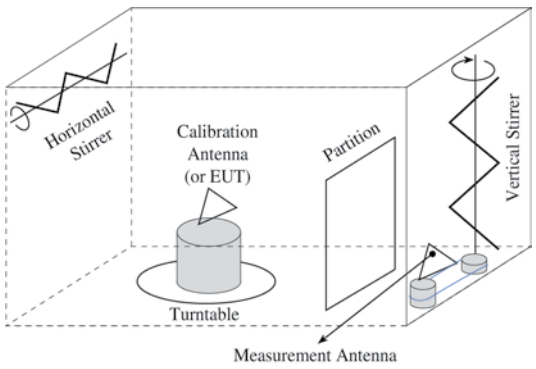

Figure 2 Illustration of practical implementation of a reverberation chamber

Chamber Calibration

Before using a reverberation chamber as shown in Figure 2, the loss factor, i.e. the chamber transfer function, between of the locations of the calibration antenna and the measurement antenna has to be characterized. In other words, the chamber needs to be calibrated before any measurement can take place. A network analyzer is typically used to perform the calibration. During calibration, the stirrers and the turntable, being set to the same speeds that will be used during the EUT measurement, rotate continuously, and sufficient samples of the S_{21} reading are taken. The measured chamber transfer function, called gain factor (G),

is then calculated as the average of the magnitude over all the S_{21} samples.

$$G = (|S_{21}|^2) \tag{21}$$

Expressed in decibel unit, (21) can be written as,

$$G_{dB} = 10\lg(|S_{21}|^2) \tag{22}$$

The mismatch of the measurement antenna will be obtained by averaging the samples of measured return loss. If the measurement antenna is connected to port 1 of the network analyzer, the mismatch is then calculated as,

$$m_{dB} = 10\lg\left(\frac{1}{1-|(S_{11})|^2}\right) \tag{23}$$

The overall correction factor (CF) is the summation of the gain factor and the mismatch factor, that is,

$$CF = G_{dB} + m_{dB} \tag{24}$$

Ideally, all the RF energy needs to be coupled through resonance modes such that the average of all S_{21} samples should be zero. However, there is always a slight unstirred component of direct coupling. Any unstirred energy not subject to the same Rayleigh fading can be better represented by a Rician distribution. This component of unstirred power can be measured simply by taking the average over S_{21} samples, i.e. $|(S_{21})|^2$. Note that this is different from G, for which the average is taken over the magnitude of samples, i.e. $|(S_{21})|^2$. And the figure of merit, denoted as Rician K factor, to characterize the level of the system imperfection can be given as,

$$K = \frac{|(S_{21})|^2}{(|S_{21} - (S_{21})|^2)} \tag{25}$$

Figure 3 displays a typical performance measurement of the reverberation chamber calibration data. The red trace shows the correction factor in decibel unit, while the green is the K factor.

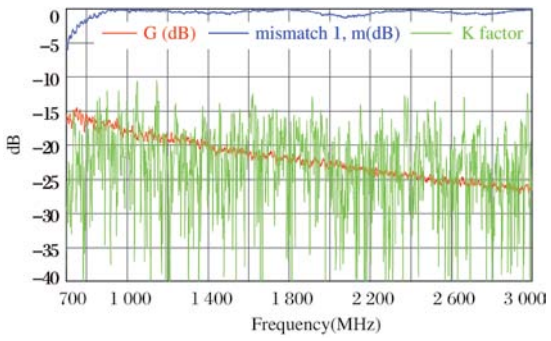

Figure 3 Measured gain factor, mismatch and factor for ETS-Lindgren AMS7000 system

TRP Measurement

Figure 4 shows the system setup for performing a total radiated power (TRP) measurement. The EUT is placed on the top of the turntable approximately at the location where the calibration antenna was set. During the measurement, the EUT is set to transmit maximum power by the communication tester, while the receiver samples the power readings.

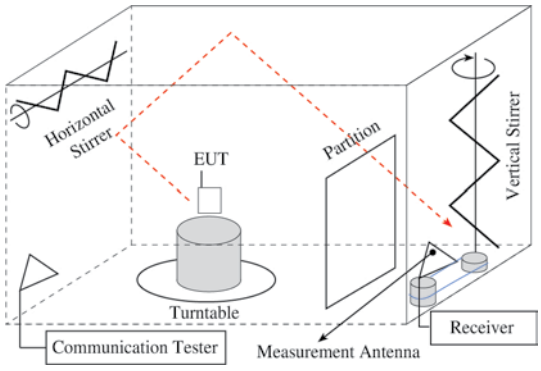

Figure 4 Illustration of the practical implementation of a reverberation chamber for TRP measurements

As shown in Figure 5, the red trace represents the received power samples that look seemingly random, while the average achieves a rather stable constant after about 300 samples being collected. The average is corrected with the factor obtained in (24) to obtain the final result.

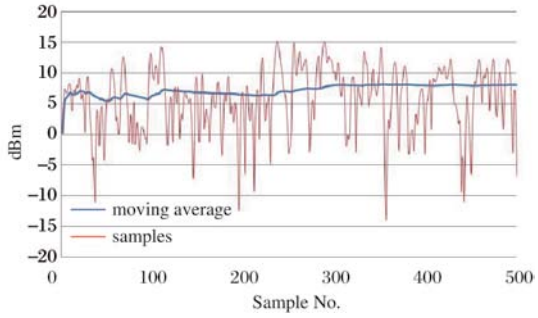

Figure 5 Measured TRP data from AMS7000 system

TRS Measurement

Figure 6 shows the system setup for performing total radiated sensitivity (TRS) measurements. During the measurement, the EUT is placed at the same location, and the measurement antenna transmits base station power to the EUT through resonance modes. The dotted line indicates the direction of one particle that bounces from the measurement antenna to the EUT. Although the measurement direction is reverse in TRS, in contrast to TRP, the reciprocity of the system prevails. Thus, the same chamber correction factor used in TRP is applicable for TRS as well. The

testing procedure is defined in two steps. First, the ensemble of the measurement is not taken from the sensitivity measurement, but from the received signal strength (RSS) readings. The base station outputs a fixed level of downlink power to which the EUT reports RSS values back to the communication tester in real time. After sampling enough RSS values, the relationship of the base station power to the reported RSS can be obtained. Second, after RSS sampling, several sensitivity measurements are taken while the chamber is not stirred. Since sensitivity measurements are not taken in the state of statistical uniformity, these EIS results need to be normalized with the relationship of RSS to the given base station power that we characterized in the first step.

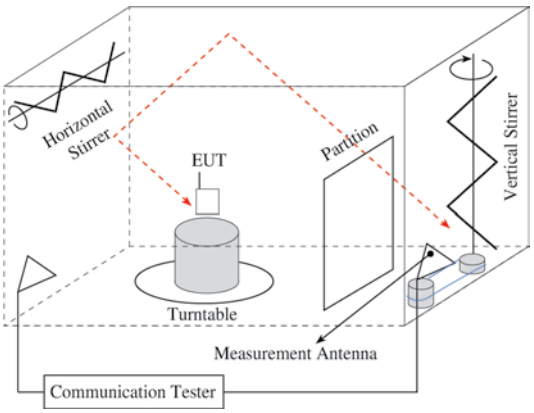

Figure 6 Illustration of the practical implementation of a reverberation chamber for TRS measurements

As shown in Figure 7, the red trace represents the reported RSS samples, the average of which achieves a rather stable constant after about 200 samples being collected.

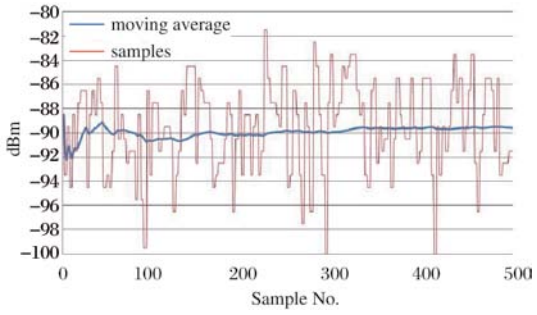

Figure 7 Measured RSS data from an AMS7000 system

Reverberation Chambers in MIMO Applications

Reverberation chambers are regarded as one of the test environments suitable for MIMO measurements due to their inherent nature of fading characteristic. However, one important fact about MIMO measurement is that its performance is a function of the operating environment. One MIMO device measured in one given emulated environment will not perform the same in another emulated environment. Reverberation chambers provide one subset of such multiple-path environments, which are emulated in terms of frequency fading, spatial diversity and temporal diversity. Limited by the nature of its statistical uniformity, inside reverberation chambers, the fields are well stirred, so the range of multipath environments is not easily emulated. In addition, the angles of arrival are such uniformly distributed that removes the ability to evaluate pattern diversity. The temporal diversity may only be emulated with the addition of the instrumentation for channel emulation that can feed faded signals in different temporal steps[9].

Connected to the two antennas for downlink, the communication tester measures data throughput, while the chamber is being stirred. Quite a large quantity of packets need to be sent to the EUT so that the test time is sufficiently long enough and the turntable can make one entire rotation at a given power level. Figure 8 shows the test setup for MIMO.

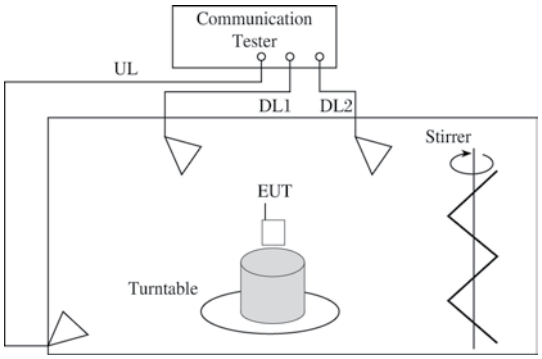

Figure 8 Illustration of a practical implementation of a reverberation chamber for MIMO measurements

Summary

The main principle of using reverberation chambers as a measurement system originates from its chamber transfer function, which is deduced from both wave-like and mode-like perspectives. Once the chamber transfer function has been characterized, we can use the system to perform either TRP/TRS measurements for SISO, or throughput measurement for MIMO.

Although the repeatable statistical behavior has been utilized for radiated measurements, reverberation chambers are inadequate for characterizing radiated pattern geometry. The inability for measuring the antenna pattern is recognized as the shortcoming for

reverberation chambers. However, there has been some research work conducted to explore the possibilities for measuring the antenna pattern in reverberation chambers[10]. Another possibility to measure the antenna pattern is to excite known resonance modes from a basis to characterize the antenna in K-space, which subsequently is transferred into pattern geometry through the Fourier transform. Such a concept is similar to what has been applied in magnetic resonance imaging (MRI). However, the difficulty is how to control the modes to be excited inside reverberation chambers. More research will need to be explored in order to understand the practicality of such methodology.

Acknowledgement

The authors would like to recognize and thank Guo Lin with the China Academy of Telecommunication Research (CATR) of MIIT in Beijing, China and William F. Young, Ph.D. with the RF Fields Group at the National Institute of Standards and Technology (NIST) in Boulder, Colorado for their expert review of this article and constructive comments.

References

[1] P. Corona, G. Latmiral, and E. Paolini, "Performance and analysis of a reverberating enclosure with variable geometry," IEEE Trans. Electromagn.Compat.,vol. EMC-22, pp. 2-5, 1980.

[2] M. L. Crawford and G. H. Koepke, "Design, evaluation, and use of a reverberation chamber for performing electromagnetic susceptibility/vulnerability measurements," U.S. Nat. Bur. Stand. Tech. Note 1092, 1986.

[3] K. Rosengren, P.-S. Kildal, C. Carlsson, and J. Carlsson, Characterization of antennas for mobile and wireless terminals in reverberation chambers: improved accuracy by platform stirring, Microwave Opt.Technol. Lett., vol. 30, no. 20, pp. 391-397, Sep. 2001.

[4] M. Lienard and P. Degauque, "Simulation of dual array multipath channels using mode-stirred reverberation chambers,"Electron. Lett., vol. 40, no. 10, pp. 578-579, May 2004.

[5] David Hill, "Reciprocity in Reverberation Chamber Measurements,"IEEE Trans. Electromagn. Compat., pp. 117-119, VOL. 45, NO. 1, Feb. 2003.

[6] D. A. Hill, M. T. Ma, A. Ondrejka, B. F. Riddle, M. Crawford, and R. Johnk, "Aperture excitation of electrically large, lossy cavities,"IEEE Trans. Electromagn. Compat., vol. 36, no. 3, pp. 169-178, 1994.

[7] David Hill, Electromagnetic Fields in Cavities: Deterministic and Statistical Theories, Sep. 2009.

[8] Philippe Besnier, Bernard Demoulin, Electromagnetic Reverberation Chambers, Sep. 2011.

[9] Wright, C., "Utilizing a channel emulator with a reverberation chamber to create the optimal MIMO OTA test methodology," Global Mobile Congress, 2010.

[10] Garcia-Fernandez, M. A., "Antenna Radiation Pattern Measurements in Reverberation Chamber Using Plane Wave Decomposition,"IEEE Trans. Antenna Propagation, pp. 5000-5007, VOL. 61, October 2003.

Yulung Tang is the regional director for test solutions at ETS-Lindgren, located in Taipei, Taiwan. He received his M.S. in Electrical Engineering from California Institute of Technology in 2004. During his studies in school, he conducted research work on the MMIC development for radio astronomy applications, as well as mmW point-to-point communication systems. He joined TriQuint Semiconductor in 2005 as a design engineer, working on the MMIC development for wireless communication systems. Mr. Yang has been with ETS-Lindgren since 2008, working primarily on the RF design of anechoic and reverberation chambers, as well as antenna measurement systems. His interest of research is focused on RF circuit and system design for radio astronomy, electromagnetic wave measurement and medical applications. He may be reached at Yulung.Tang@ets-lindgren.com.

Chengshao yang is an RF engineer with ETS-Lindgren, located in Beijing, China. He received his Engineering Master Degree from Communication University of China in 2011. He recently joined ETS-Lindgren to address Over-The-Air (OTA) anechoic chamber and reverberation chamber wireless testing system integration. Mr. Cheng provides technical support to ETS-Lindgren customers. He has successfully completed more than 20 wireless testing systems. His wireless testing experience includes helping customers with the challenges of a CTIA audit. He may be reached at Cheng.Shaoyang@ets-lindgren.com.

Jiang Xiao is an RF design engineer at ETS-Lindgren, located in Beijing, China. He has more than seven years of experience in RF testing, EMC/OTA chamber and system design, and antenna design and measurements. Dr. Xiao received his Ph.D. degree in electronics engineering from Chinese Academy of Sciences, China in 2006. From 2008-2011 he studied at the EMC Center of the Missouri University of Science and Technology in Rolla, Missouri. He has published more than 10 papers in the IEEE Transactions on Electromagnetics and in international conference proceedings. He may be reached at John.Xiao@ets-lindgren.com.